



A Simulation-Aided LCL Filter Design for Grid-Interactive Three-Phase Photovoltaic Inverters

Ali Mazaheri^a, Farhad Barati^{b,*} Majid Jamil^c

^{a,b,c}Division of Energy, Materials and Energy Research Center, Karaj, Iran

ARTICLE INFO

Received: 26 June 2019

Received in revised form:

16 September 2019

Accepted: 17 September 2019

Available online:

Keywords:

PV, Grid-Interactive Inverters, LCL filter, Simulation-Aided Design.

ABSTRACT

Photovoltaic (PV) inverters, as the key technology for integrating PVs into the grid, are increasingly gaining importance. The two-level three-phase topology is the basic topology for such inverters. It produces lots of harmonics which necessitates significant suppressions prior to be connected to the grid. The LCL filter is known as an effective topology in significantly attenuating harmonics with small filter components. In this paper, we propose a simulation-aided design for the LCL filter to be employed in grid-interactive PV inverters. Starting from some initial values for the filter parameters, the proposed approach imposes analytical as well as simulation constraints. Simulations, performed in Matlab/Simulink, are repeated as long as the Total Harmonics Distortions (THD) in the injected current to grid reaches its limit, i.e. THD=5%. As a design goal, attempts are made to reduce inductors' sizes, since they are voluminous and sources for Electromagnetic Interferences (EMI). Simulations are provided both for the inverter mode in which some active power is injected to the grid and for the active rectifier mode in which some active power is absorbed from the grid.

© 2019 Published by University of Tehran Press. All rights reserved.

1. Introduction

PV inverters are classified into off-grid, grid-tied, and grid-interactive ones. Off-grid PV inverters, as implies, have no connection to the utility grid while grid-tied and grid-interactive PV inverters do have connections to the utility grid. A grid-tied PV inverter is employed to inject the PV array's power to the grid while a grid-interactive PV inverter is able to both inject and absorb the active power from the grid. It is employed where the PV system is accompanied by energy storage elements and local loads such as in a microgrid [1, 2]. In Figure 1, a grid-interactive PV system is shown. It is clear that, the inverter can run either in the inverter mode in which the power is injected

to the grid or in the active rectifier mode in which the power is absorbed from the utility grid [3, 4].

The two-level three-phase topology is the basic topology employed for PV inverters. It benefits from a simple structure and control compared to higher level ones [5-7]. The two-level three-phase inverter, however, produces lots of harmonics at its output voltage. So, the employment of a power filter between the inverter and the grid is necessary [8-11]. The power filter must attenuate harmonics produced by the inverter such that the injected current to grid THD satisfies the grid codes. The codes, in fact, necessitate a $\text{THD} < 5\%$ for the injected current to grid [12].

Different filter topologies are already employed for PV inverters. They include L, LC, and LCL filters. They

*Corresponding Author's E-mail address: f.barati@mserc.ac.ir

are of the 1st, 2nd, and 3rd orders, respectively. As compared with the L and LC filters, the LCL filter is known to provide significant attenuations with small filter components. To stabilize the LCL filter performance, different passive and active damping techniques are already presented. An active damping is included in the control system which stabilizes the filter performance with no losses introduced.

In [13, 14], design methods are presented for LCL and LLCL filters to be employed in single-phase grid-tied PV inverters. A coupled inductance design for LC and LCL filters is presented for single-phase grid-tied inverters in [15]. In [16], a LCL filter design for a multi-megawatt medium-voltage converter for offshore wind turbines is presented. An approach for the LCL filter design for three-phase off-grid PV inverters is presented in [17].

Nowadays, powerful simulation tools such as Matlab/Simulink and PSCAD/EMTDC are available which can predict the behaviour of power electronics systems accurately. They can perform as design tools; instead of the conventional design approaches which are based only on analytical expressions. Analytical expressions, to be easy enough to work with by hand, are not accurate enough [18].

This paper proposes a simulation-aided design which combines both of the simulation and analytical tools for the LCL filter. Through the design procedure, the proposed approach imposes analytical as well as simulation constraints. As the main simulation constraint, the injected current to grid's THD must be below the limit. Attempts are made to reduce inductors' sizes as much as possible to obtain a small filter with low EMI introduced.

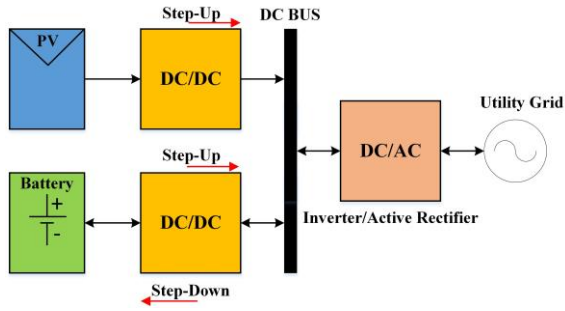


Figure 1. A grid-interactive PV system

2. LCL Filter at the Fundamental Component

For PV applications, the most appropriate inverter topology is the basic one, i.e. the two-level three-phase topology. A single two-level three-phase inverter is suitable for low power PVs while, for high powers, a

number of them need to be employed in parallel. The two-level topology, however, produces lots of harmonics which need to be significantly attenuated before connecting to the grid. The LCL filter, as explained earlier, is among the most effective topologies which significantly attenuates harmonics at small filter components [19]. The single-phase diagram of the two-level grid-interactive inverter with the LCL filter is shown in Fig.2.

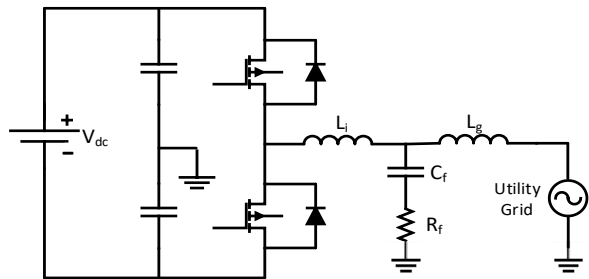


Figure 2. Single-phase diagram of the two-level grid-interactive inverter with the LCL filter

We want the parallel branch in the LCL filter, i.e. the filter capacitor in series with the damping resistor, as a path only for harmonics. In other words, at the fundamental component, our design is performed such that the parallel branch can be approximately considered as open-circuited. Based on this assumption, at the fundamental component, the LCL filter behaves such as the L filter as shown in Fig.3 in which $L_t = L_i + L_g$ is the total inductance between the inverter and the grid. In this figure, V_i is the inverter's fundamental component voltage at an angle of δ^0 with respect to the grid voltage. Based on the equivalent-circuit, one can write:

$$V_i(\angle \delta^0) = V_g(\angle 0^0) + jX_t I_g \quad (1)$$

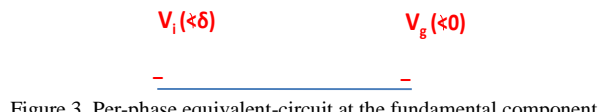
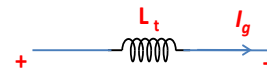


Figure 3. Per-phase equivalent-circuit at the fundamental component

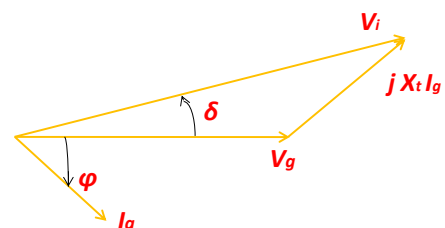


Figure 4: Phasor diagram at the fundamental component

A phasor diagram as shown in Fig.4 can be depicted for equation (1). In this figure, I_g lags V_g meaning that some reactive power is exported to the grid. A higher voltage needs to be produced by the inverter when, besides the active power, the reactive power is exported to the grid too. One can write the exchanged active and reactive powers with the grid as follows.

$$P = \frac{3}{2} \frac{V_i V_g}{X_t} \sin(\delta) \quad (2-a)$$

$$Q = \frac{3}{2} \frac{V_g}{X_t} (V_i \cos(\delta) - V_g) \quad (2-b)$$

3. Proposed Simulation-Aided Design for the LCL Filter

In this section, the proposed simulation-aided design for the LCL filter is presented. We start from the equivalent-circuit for non-fundamental components as shown in Fig.5. Note that, in this figure, the grid is considered to be harmonics free and therefore, the grid side of the filter is short-circuited. In this figure, V_h denotes the h^{th} harmonics of inverter's output voltage, I_{hi} and I_{hg} are the h^{th} harmonics of inverter and grid currents, respectively. The Sinusoidal Pulse-Width Modulation (SPWM) is chosen. In such case, it is known that, the lowest harmonics components are located around ω_c which is the switching angular frequency.

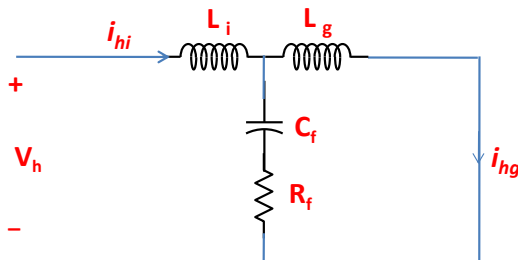


Figure 5: Non-fundamental component per-phase equivalent-circuit

Whereas the fundamental frequency, we want the parallel branch at the switching frequency, as well as higher frequencies, to absorb significant amounts of currents. In this way, small amounts of harmonics components are injected to the grid. For this purpose, the following needs to be satisfied.

$$L_g \omega_c \ll \sqrt{R_f^2 + \frac{1}{(C_f \omega_c)^2}} \quad (3)$$

By satisfying the above relation for the switching frequency, it is clear that, it will be satisfied for higher frequencies as well. We also want to limit the

inverter's output current harmonics since, in this way, less core losses are introduced in the inverter side inductor. For such purpose, we need to satisfy the following.

$$|Z| = \sqrt{R_f^2 + (L_g \omega_c - \frac{1}{C_f \omega_c})^2} \ll 1 \quad (4)$$

The above relation implies that for the switching frequency, and of course higher frequencies, the resulting filter impedance Z is high enough to significantly attenuate harmonics produced by the inverter.

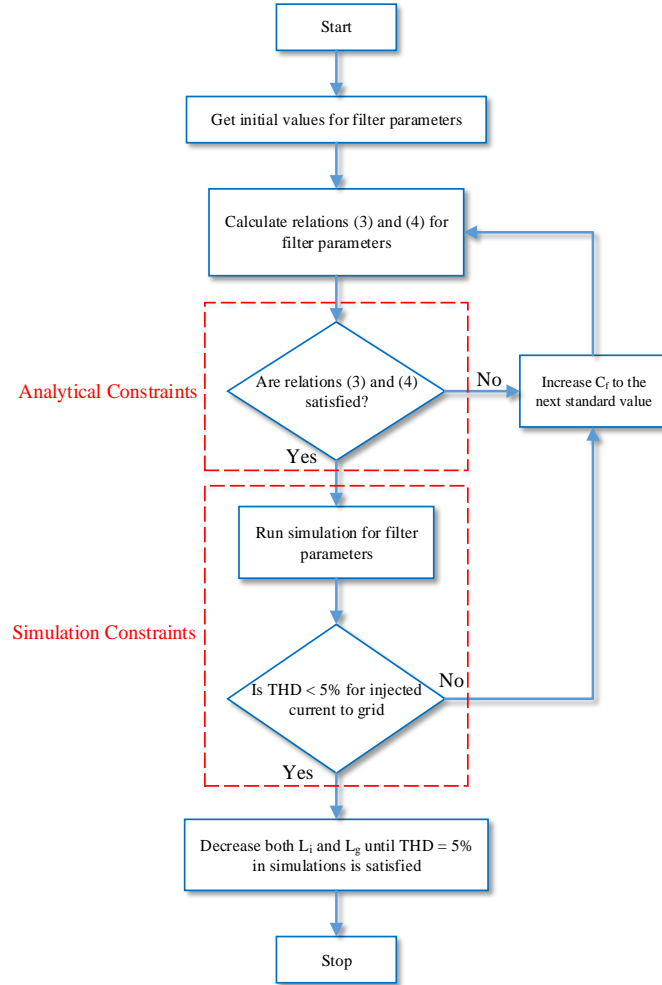


Figure 6: Proposed simulation-aided design algorithm flowchart

The proposed design approach algorithm is depicted in a flowchart as in Fig.6. As can be seen, the algorithm starts from some typical initial values for the LCL filter parameters. The relations (3) and (4) are then evaluated for the filter parameters. We want to evaluate if both of the relations are satisfied. If this is not the case, the next step is to increase the

filter capacitance, i.e. C_f , to the next standard value. In fact, in the proposed approach, we prefer to increase the filter capacitance if the filter attenuation is not high enough. For the new filter parameters, again, the relations (3) and (4) are calculated and evaluated. This procedure is repeated until both of the relations are satisfied.

The LCL filter whose parameters have satisfied the relations in (3) and (4) is then evaluated in simulations. As described earlier, we employ simulations as an accurate tool for the evaluation of filter performance. Specifically, we evaluate the filter performance in simulations in terms of the injected current to grid THD which should satisfy the grid code. If the requirement $\text{THD} < 5\%$ is not satisfied, our preference is, again, to increase the filter capacitance to the next standard value. This procedure must be repeated until the THD requirement in simulations is satisfied.

The LCL filter whose parameters have satisfied both of the analytical and simulations constraints might be a large one. So, we might be able to make it smaller. To make the filter smaller, our preference is to reduce the filter inductors' values. As described earlier, they are voluminous, heavy, and sources for EMI. Therefore, any reduction in their sizes is desired. We start reducing both of the inverter side and grid side inductors until the $\text{THD}=5\%$ is reached in simulations.

4. A Case Study

In this section, the proposed approach is employed for an inverter with the parameters listed in Table 1. Some typical initial values for the filter parameters are considered as in Table 2. According to the design algorithm, at first, we have to evaluate the analytical constraints as in the relations (3) and (4). For the initial values, one can calculate that

$$L_g \omega_c = 62.8\Omega \text{ while } \sqrt{R_f^2 + \frac{1}{(C_f \omega_c)^2}} = 1.9\Omega \text{ which}$$

confirms the correctness of the relation in (3). Also, for the relation in (4), it can be calculated that $|Z|=125\Omega$ which is much higher than the unity. So, as seen, the analytical constraints are satisfied very well.

Now, we have to evaluate the LCL filter in simulations. The simulations are performed in Matlab/Simulink. Using the simulations, the THD for the injected current to grid is evaluated in order to satisfy the requirement $\text{THD} < 5\%$. Based on the simulations, it is seen that the injected current to grid has a $\text{THD} = 1\%$ which is far below the limit. This implies that the filter is a large one and therefore, we are able to reduce its dimensions. We start to reduce the inductors' values until a $\text{THD} = 5\%$ is reached in simulations. These values are considered as the filter final parameters which are listed in Table 3.

In the following, the stability and performance analysis of the designed filter are presented. Based on the equivalent circuit in Fig.2, a transfer function can be derived from the inverter's output voltage to the current injected to the grid. It is as follows.

$$H(s) = \frac{I_g(s)}{V_{pwm}(s)} \quad (5)$$

Where, $I_g(s)$ and $V_{pwm}(s)$ are the Laplace transformations of injected current to grid and inverter's output voltage, respectively. Note that, $H(s)$ is derived based on the superposition principle which, for its derivations, the grid voltage is not included. One can derive:

$$H(s) = \frac{R_f C_f + 1}{L_i L_g C_f s^3 + R_f C_f (L_i + L_g) s^2 + (L_i + L_g) s} \quad (6)$$

4.1 Stability Analysis

As seen, $H(s)$ is a 3^{rd} order transfer function; showing the three storage elements exist in the circuit. It can also be seen that without a damping resistor, i.e. $R_f = 0$, the filter behaves oscillatory. In the other words, by employing the damping resistor, the filter can be appropriately stabilized. One can rewrite the transfer function in (6) in the standard form as in the following.

$$H(s) = \frac{1}{L_i L_g C_f s} \frac{1}{s^2 + \frac{R_f}{L_i L_g} (L_i + L_g) s + \frac{(L_i + L_g)}{L_i L_g C_f}} \quad (7)$$

Table 1: Parameters of a grid-interactive inverter

Parameter	Value
f_c	10 kHz
$V_{g(L-L)}$	400 Vrms
Nominal Apparent Power	10 KVA
f_g	50 Hz

Table 2: Typical initial values for the LCL filter parameters

Parameter	Description	Value
L_i	Inverter side inductor	1mH
L_g	Grid side inductor	0.5mH
C_f	Filter capacitor	47μF
R_f	Damping resistor	10Ω

Table 3: Final values for the LCL filter parameters

Parameter	Description	Value
L_i	Inverter side inductor	0.2mH
L_g	Grid side inductor	0.1mH
C_f	Filter capacitor	470μF
R_f	Damping resistor	10Ω

In the derivations of above equation, it is assumed that the term $R_f C_f + 1 \approx 1$, since C_f takes very small values. Based on the equation in (7), the filter's natural frequency and damping ratio can be calculated as follows.

$$\omega_n = \sqrt{\frac{1}{C_f} \left(\frac{1}{L_i} + \frac{1}{L_g} \right)} \quad (8-a)$$

$$\zeta = \frac{R_f}{2} \sqrt{C_f \left(\frac{1}{L_i} + \frac{1}{L_g} \right)} \quad (8-b)$$

For the final filter parameters as listed in Table 3, it can be calculated that the transfer function's poles are located at $S_1 = 0$ and $S_{2,3} = -4.2 \times 10^3 \pm j4.2 \times 10^4$. It is clear that, one of the poles is located at the origin and the two others are located in the left hand side far from the imaginary axis. So, it can be concluded that, in terms of the stability, we have achieved a very well designed filter.

4.2

4.3 Performance Analysis

The Bode diagram of transfer function $H(s)$ for the final filter parameters is shown in Fig.7. We know that, the inverter's output voltage comprises the fundamental component at $\omega_g = 100\pi \frac{rad}{s}$ and harmonics components whose lowest are located

around $\omega_c = 1.25 \times 10^5 \frac{rad}{s}$ as the switching angular frequency. As can be seen, the injected current to grid lags the inverter's output voltage in the low frequency range, where the fundamental frequency is located, by 90°.

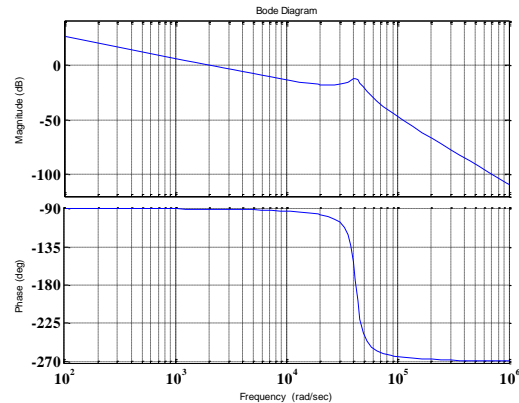


Figure 7: Bode diagram of $H(s)$ for the LCL filter with final parameters

This implies that, for the fundamental component, the designed LCL filter behaves such as the L filter. In the other words, at the fundamental component, the parallel branch is approximately open-circuited which verifies the design objectives as described in section 2. Also, at the switching frequency, the designed LCL filter provides significant attenuations. As can be seen, an attenuation of at least -50dB for the inverter's output voltage harmonics is achieved. Such attenuation means that the filter provides a significant suppression of harmonics resulting in waveforms close to the sinusoidal for the injected current to grid. Also, it can be seen that, at the filter's natural frequency, i.e. $\omega_n = 4.2 \times 10^4 \frac{rad}{s}$, an attenuation of about -20dB is achieved. This confirms the effectiveness of damping resistor employed.

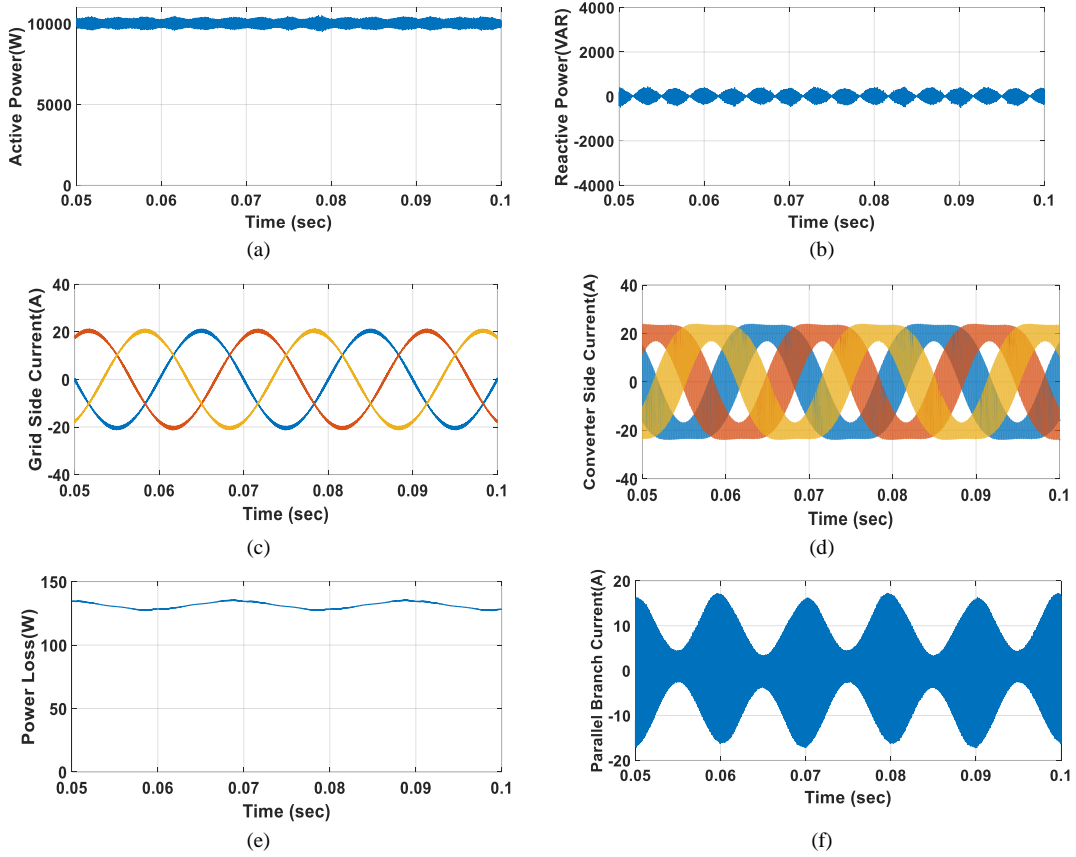


Figure 8: Simulation results for the inverter mode

5. Simulations

In this section, the simulation results with the final LCL filter parameters are presented. Simulations are performed in Matlab/Simulink for the grid-interactive inverter equipped by a closed-loop vector control system. The closed-loop vector control system regulates the exchanged active and reactive powers with the grid according to their reference values. To utilize the nominal inverter's apparent power for the active power, we set the reference value for the reactive power to zero.

5.1 Inverter Mode

In this mode, it is set to inject 10kW power to the grid. The results are shown in Figure 8. They are shown for steady-state. As seen, the injected currents to grid are close to sinusoidal with the $\text{THD} \approx 5\%$.

Based on the parallel branch current, the mean total power loss of filter which occurs in the damping resistors is shown. It is equal to 132W. This power loss means an efficiency of 98.7% for the filter in the inverter mode. This confirms that in the filter final design, while attaining appropriate stability, the efficiency is not sacrificed.

5.2 Active Rectifier Mode

In this mode, it is set to absorb 10kW power from the grid. The results are shown in Figure 9. They are shown for steady-state. It is seen that the results are very close to the inverter mode, except the power loss in damping resistors. In fact, the mean total power loss in damping resistors equals to 139W in the active rectifier mode. This means an efficiency of 98.6% for this mode which confirms that, while attaining appropriate stability, the filter efficiency is not sacrificed.

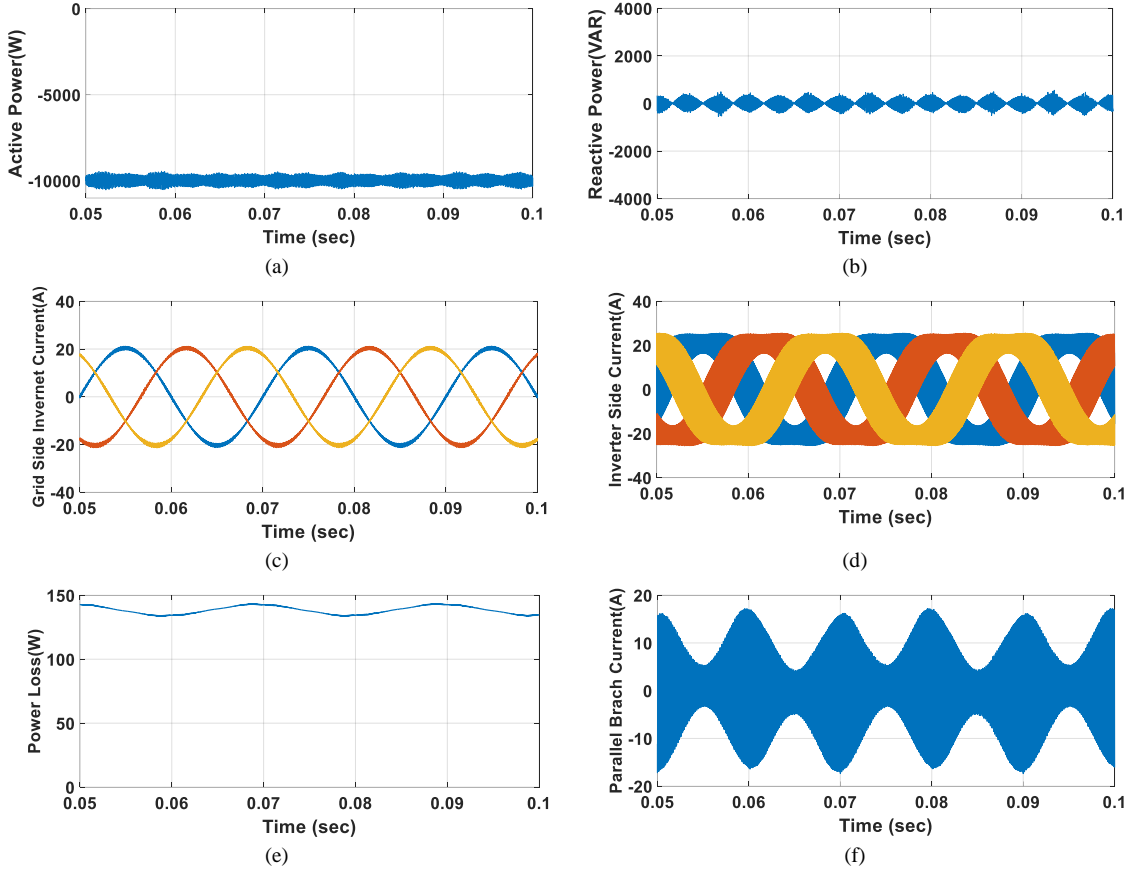


Figure 9: Simulation results for the active rectifier mode

6. Conclusions

The proposed simulation-aided design for the LCL filter presents an approach which, besides the analytical constraints, effectively employs the simulations in Matlab/Simulink. The analytical constraints imposed are sufficient in obtaining appropriate filter parameters in terms of the injected current to grid THD. These constraints, however, may not be necessary meaning that smaller filter dimensions may still satisfy the requirement THD < 5%. We employed the simulations to reduce the filter dimensions until the THD reaches the limit. In this procedure, the emphasis is on reducing the inductors' sizes as much as possible, since they are voluminous and sources for EMI. We, of course, during the procedure, proposed to increase the filter's capacitor size if needed.

Acknowledgement

This work was supported by Materials and Energy Research Centre, Karaj, Iran.

Nomenclature

L_t	total inductance between inverter and grid
ω_c	switching angular frequency
ω_g	grid angular frequency

References

- [1] E. Bullich-Massagué, M. Aragüés-Peñaiba, A. Sumper, and O. Boix-Aragones, "Active power control in a hybrid PV-storage power plant for frequency support," *Solar Energy*, vol. 144, pp. 49-62, 2017.
- [2] Y. Riesen, C. Ballif, and N. Wyrsch, "Control algorithm for a residential photovoltaic system with storage," *Applied Energy*, vol. 202, pp. 78-87, 2017.
- [3] A. Mazaheri, F. Barati, and F. Ghavipanjeh, "Multi-variable PI control design for grid-tied three-phase PV inverters," *IEEE Int. Conference on Renewable Energy and Distributed Generation (ICREDG)*, pp. 1-4, 2019.
- [4] S. Dhar and P. K. Dash, "Adaptive backstepping sliding mode control of a grid interactive PV-VSC system with LCL filter," *Sustainable Energy, Grids and Networks*, vol. 6, pp. 109-124, 2016.
- [5] Y. Ando, T. Oku, M. Yasuda, Y. Shirahata, K. Ushijima, and M. Murozono, "A compact SiC photovoltaic inverter with maximum power point tracking function," *Solar Energy*, vol. 141, pp. 228-235, 2017.
- [6] L. Hassaine, E. Olias, J. Quintero, and V. Salas, "Overview of power inverter topologies and control structures for grid connected photovoltaic systems," *Renewable and Sustainable Energy Reviews*, vol. 30, pp. 796-807, 2014.
- [7] P. M. Rodrigo, R. Velázquez, and E. F. Fernández, "DC/AC conversion efficiency of grid-connected photovoltaic inverters in central Mexico," *Solar Energy*, vol. 139, pp. 650-665, 2016.
- [8] M. Büyük, A. Tan, M. Tümay, and K. Ç. Bayındır, "Topologies, generalized designs, passive and active damping methods of switching ripple filters for voltage source inverter: A comprehensive review," *Renewable and Sustainable Energy Reviews*, vol. 62, pp. 46-69, 2016.
- [9] Y. Du, D. D.-C. Lu, G. James, and D. J. Cornforth, "Modeling and analysis of current harmonic distortion from grid connected PV inverters under different operating conditions," *Solar Energy*, vol. 94, pp. 182-194, 2013.
- [10] N. F. Guerrero-Rodríguez, A. B. Rey-Boué, L. C. Herrero-de Lucas, and F. Martínez-Rodrigo, "Control and synchronization algorithms for a grid-connected photovoltaic system under harmonic distortions, frequency variations and unbalances," *Renewable Energy*, vol. 80, pp. 380-395, 2015.
- [11] M. I. Hamid and A. Jusoh, "Reduction of waveform distortion in grid-injection current from single-phase utility interactive PV-inverter," *Energy Conversion and Management*, vol. 85, pp. 212-226, 2014.
- [12] IEEE Standard for interconnecting distributed resources with electric power systems, *IEEE*, 2008.
- [13] M. Monfared and M. Sanatkar, "Design of LCL and LLCL filters for single-phase grid connected converters," *IET Power Electronics*, vol. 9, 2016.
- [14] W. Wu, Y. He, T. Tang, and F. Blaabjerg, "A new design method for the passive damped LCL and LLCL filter-based single-phase grid-tied inverter," *IEEE Transactions on Industrial Electronics*, vol. 60, pp. 4339-4350, 2013.
- [15] W. Chen and B. Jiang, "Coupled inductance design for grid-connected photovoltaic inverters," *IET Power Electronics*, vol. 8, pp. 2204-2213, 2015.
- [16] M. Zabaleta Maeztu, E. Burguete, D. Madariaga, I. Zubimendi, M. Zubia, and I. Larrazabal, "LCL grid filter design of a multi-megawatt medium-voltage converter for offshore wind turbine using SHEPWM modulation," *IEEE Transactions on Power Electronics*, vol. 31, 2015.
- [17] M. K. Javid and F. Barati, "An LCL filter design for three-phase off-grid PV inverters," *Journal of Solar Energy Research*, vol. 3, pp. 29-33, 2018.
- [18] R.A.Dougal, "Simulation methods for design of networked power electronics and information system," *Technical Report*, 2014.
- [19] Y. Liu, P. Jianchun, W. Guibin, W. Huazhi, and K. Y. See, "THD and EMI performance study of foil-wound inductor of LCL filter for high power density converter," *IEEE International Power Electronics and Motion Control Conference*, 2016, pp. 3467-3471.